Original Article

Clinical and histological findings of autosomal dominant renal-limited disease with *LMX1B* mutation

Takao Konomoto[1], Hideaki Imamura[1], Mayuko Orita[1], Etsuko Tanaka[2], Hiroshi Moritake[1], Yuji Sato[3], Shouichi Fujimoto[3, 4], Yutaka Harita[5], Satoshi Hisano[6], Koh-ichiro Yoshiura[7], Hiroyuki Nunoi[1]

[1]Division of Pediatrics, Department of Developmental and Urological-Reproductive Medicine, Faculty of Medicine, University of Miyazaki, Miyazaki, Japan

[2]Department of Pediatrics, Miyazaki Prefectural Miyazaki Hospital, Miyazaki, Japan

[3]Dialysis Division, University of Miyazaki Hospital, Miyazaki, Japan

[4]Department of Hemovascular Medicine and Artificial Organs, University of Miyazaki, Miyazaki, Japan

[5]Department of Pediatrics, Graduate School of Medicine, The University of Tokyo, Tokyo, Japan

[6]Department of Pathology, Faculty of Medicine, Fukuoka University, Fukuoka, Japan

[7]Department of Human Genetics, Graduate School of Biomedical Sciences, Nagasaki University, Nagasaki, Japan

Contribution: Konomoto T, Nunoi H, and Fujimoto S designed the experiments; Konomoto T, Imamura H, Orita M, Tanaka E, and Sato Y participated in clinical data collection; Hisano S performed renal histological analysis; Harita Y performed immunohistochemical analysis of podocyte protein; Nunoi H and Moritake H, provided technical support; Konomoto T performed Sanger sequencing and wrote the manuscript; Yoshiura K performed whole exome sequencing and analyzed data.

Correspondence: Takao Konomoto

Division of Pediatrics, Department of Developmental and Urological-Reproductive Medicine, Faculty of Medicine, University of Miyazaki, 5200 Kihara, Kiyokake-cho, Miyazaki 889-1692, Japan

E-mail: konomoto@med.miyazaki-u.ac.jp

Phone: +81-985-85-0989, Fax: +81-985-85-2403

Short running title: Renal-limited disease with *LMX1B* mutation

ABSTRACT

Aim Mutations of *LMX1B* cause nail-patella syndrome, a rare autosomal dominant disorder. Recently, *LMX1B* R246Q heterozygous mutations were recognized in nephropathy without extra-renal manifestation. The aim of this study was to clarify characteristics of nephropathy caused by R246Q mutation.

Methods Whole exome sequencing was performed on a large family with nonsyndromic autosomal dominant nephropathy without extra-renal manifestation. Clinical and histological findings of patients with *LMX1B* mutation were investigated.

Results *LMX1B* R246Q heterozygous mutation was identified in five patients over three generations. Proteinuria or hematoproteinuria was recognized by urinary screening from all patients in childhood. Proteinuria gradually increased to nephrotic levels and renal function decreased in adolescent. Two patients progressed to end stage renal disease in adulthood. Renal histology demonstrated minimal change in childhood and FSGS in adulthood. Focal collagen deposition can be detected in glomeruli even when "moth-eaten appearance" was not apparent in GBM in electron microscopy. In addition, Podocin expression in glomerular podocytes was significantly decreased even in early stage of disease progression.

Conclusions Comprehensive genetic analyses and collagen or tannic acid staining might be useful for diagnosis of *LMX1B*-associated nephropathy. While renal prognosis of R246Q may be worse than that of typical NPS nephropathy, signs of podocytepathy can be detected in infantile period, and childhood urinary screening may help an early detection.

Keyword: autosomal dominant, LMX1B, nail-patella syndrome, podocin, whole exome sequencing

Introduction

LIM homeobox transcription factor 1 beta (LMX1B) plays crucial roles during embryonic development. Mutations in *LMX1B* gene lead to nail-patella syndrome (NPS), a rare autosomal dominant disorder associated with dysplasia of patella, nails and elbows, and iliac horn formation. While skeletal and nail abnormalities have been observed in a majority of NPS patients, renal involvement occurs in approximately 30-50% of patients with NPS[1-3]. Urinary abnormalities often manifest as asymptomatic proteinuria, but can progress to nephrotic syndrome or nephritis, and occasionally end stage renal disease (ESRD). The renal pathology of NPS is characterized by irregular thickening of the glomerular basement membrane (GBM) with type III collagen fibrils and an electron-lucent area, often referred to as a "moth-eaten appearance" [2-4]. The severity of nephropathy is known to be extremely variable both within and between families[1, 4].

Recently, *LMX1B* R246Q heterozygous mutation was identified in a patient with Nail-patella-like renal disease (NPLRD), which display typical renal pathology of NPS despite lack of the skeletal or nail abnormalities[5]. The same mutation was also identified in two large families of hereditary FSGS without extrarenal manifestation[6]. To date, clinical findings and kidney histology related to the renal-limited LMX1B nephropathy

are still largely unclear, because of the limited number of the affected patients and of the lack of chronological assessment of urinary abnormality or kidney function.

Using whole exome sequencing (WES), we identified heterozygous *LMX1B* R246Q mutation in a large family of nonsyndromic autosomal dominant nephropathy without extra-renal involvement. Clinical and pathological findings revealed characteristic changes observed even in early stage and variety of disease progression.

Methods

Study participants

A family with an apparent autosomal dominant inheritance pattern of nephropathy was included in this study. Clinical evaluation of patients included physical examination, urinalysis, renal function and renal histology, when appropriate. All study procedures were reviewed and approved by the Research Ethics Committee of the Faculty of Medicine at the University of Miyazaki, with written informed consent obtained from either patients or their parents.

Whole exome sequencing

Genomic DNA (gDNA) was extracted from blood samples using Gentra® Puregene®

Blood Kit (Qiagen, Venlo, Netherlands). Patient gDNA was enriched for WES using SureSelect Human All Exome V5 (Agilent Technologies, Santa Clara, CA, USA) according to manufacturer's protocol. Prepared libraries were sequenced in pair-end mode using a HiSeq2500 (Illumina, San Diego, CA, USA). Raw data were converted to FASTQ format by bcl2fastq Conversion Software (Illumina). NovoalignMPI software version 3.02.06 (Novocraft, Selangor, Malaysia) was used to perform read mapping and base quality score recalibration of FASTQ files. For this step, human reference genome sequence hg19/GRCh37 and single nucleotide variation (SNV) information from Single Nucleotide Polymorphism Database build 138 were downloaded from the UCSC genome browser [7] and merged. Aligned reads were sorted by Novosort software (Novocraft). Polymerase chain reaction (PCR) and optical duplication were removed by MarkDuplicates of the Picard Tools package (http://picard.sourceforge.net). Genome Analysis Toolkit (GATK) version 3.1-1 [8] was used to perform local realignment (GATK IndelRealigner) and variant call (GATK HaplotypeCaller) using an in-house workflow management tool [9]. Called SNVs and short insertion/deletion loci (indels) were selected as candidate mutations using two criteria: all patients were not reference-homozygote and all unaffected individuals were reference-homozygote. Selected SNVs and indels were annotated using ANNOVAR software [10]. Finally,

variants meeting the following criteria were selected as “deleterious”: 1) mutations leading to gain or loss of a stop codon, nonsynonymous mutation, or splice site according to gene information of GENCODE version 19 [11]; 2) allele frequencies deviating from the Complete Genomics 46 dataset of unrelated individuals [12], 1000 Genome April 2012 dataset [13] and Human Genetic Variation Database (Japanese 1,208 exome dataset) version 1.41 (http://www.genome.med.kyoto-u.ac.jp/SnpDB) equal to or less than 0.5%, or; 3) variations not included in segmental duplication [14, 15]. In addition, pathogenicity of variants was analyzed using in silico predictions from Polyphen2 (http://genetics.bwh.harvard.edu/pph2/index.shtml), Sorting Intolerant From Tolerant (SIFT) (http://sift.jcvi.org) and PROVEAN (http://provean.jcvi.org/index.php).

Target sequencing

Sanger sequencing was performed on the proband. Mutation analysis was carried out by Sanger sequencing of both strands of all exons from *WT1, ACTN4, CD2AP, TRPC6* and *INF2*, using exon-flanking primers. The entire coding region and exon-intron boundaries of genes were PCR-amplified from gDNA using KOD-Plus (Toyobo, Osaka, Japan). Products were subsequently purified and subjected to direct sequencing using BigDye® Terminator v3.1 Cycle Sequencing Kit (Applied Biosystems, Carlsbad, CA,

USA) with an automatic DNA sequencer. Candidate variants including *LMX1B* identified by WES were validated by Sanger sequencing. Primers used for *LMX1B* PCR amplification were previously described [16]. PCR-amplified products corresponding to individual candidates were purified and subjected to direct sequencing.

Renal histological analyses

Immunohistochemical analyses were performed using either frozen or paraffin-embedded sections of kidney tissue. Type I and type III collagens were stained using goat polyclonal antibodies (SouthernBiotech Birmingham, AL, USA). Tissue for electron microscopy was fixed in glutaraldehyde solution and collagen was stained by tannic acid. Immunohistochemical analysis of podocyte protein expression was performed using mouse monoclonal antibodies against human podocin, as previously described [5]. Expression of podocin was compared with age-matched samples from patients with minimal change disease (MCD), a childhood nephrotic syndrome with typical proteinuria.

Results

Identification of LMX1B mutation in a family with hereditary nephrotic syndrome

A large family of nephrotic syndrome without extrarenal manifestation attracted significant attention as it consisted of five affected patients over 3 generations and two unaffected members (Fig. 1A, Table 1). The proband (III-1) had chance proteinuria and microscopic hematuria notified by urinary screenings at 1 year of age. Proband's mother (II-2) exhibited proteinuria and hematuria in a school urinary screening performed at 6 years of age. Renal function of the mother decreased gradually and progressed to ESRD; subsequently, hemodialysis was commenced at 38 years of age. Proband's grandfather (I-1) progressed to ESRD with unknown cause at 40 years of age. Proband's aunt (II-4) and aunt's daughters (III-2 and III-3) had proteinuria detected by chance by urinary screening program at 13, 11 and 1 year of age, respectively.

To identify the causal variant, WES was performed on the entire family (five patients and two unaffected family members). Disease-causing candidate mutations were assessed by previously described criteria in method. Eleven variants in 11 genes, including *TMEM51*, *LACTBL1*, *UBR3*, *TRIM42*, *GIN1*, *SH3TC2*, *IDO2*, *FLI4*, *ZIC5*, *GP1BA*, and *LMX1B*, were selected as disease-causing candidate mutations. Amongst these genes, variant of *TMEM51, GLI4, GP1BA* and *LMX1B* were predicted as disease causing mutation from in silico predictions (supplementary table 1). *TMEM51* gene coded transmembrane protein 51, which function was largely unknown. However, this

protein did not express at kidney, further no disorders were found for *TMEM51* gene. *GLI4* gene coded GLI family zinc finger 4 protein. This protein expressed at only skin, further no disorders were found for *GLI4* gene. *GP1BA* gene was known causal gene of platelet-type von Willebrand disease (VWD), which was one of a subtype of VWD. VWD was a bleeding disorder, only became apparent on bleeding history[17]. None of our patients presented with obvious bleeding features. Therefore, *LMX1B* represented the greatest potential for causing nonsyndromic familial kidney disease. Sanger sequencing confirmed a heterozygous G-to-A mutation in exon 4 of LMX1B (c.737G>A, p.R246Q) in all affected patients, but not in the two unaffected individuals (Fig. 1B). Nonsyndromic autosomal dominant FSGS genes, including *WT1, ACTN4, CD2AP, TRPC6* and *INF2*, were analyzed by Sanger sequencing in proband, since exonic mutations were not noticed.

Clinical characterization of the affected patients

Clinical data are summarized in Table 1 and Figure 2. All patients, except grandfather (I-1), first notified with chance proteinuria or hematoproteinuria by urinary screening in childhood and none of these patients presented with obvious extra-renal clinical features, such as dysplasia of patella, nails and iliac horn formation (Fig. 1B). Hematuria was

observed in all patients at last follow up. Renal histological examination of the proband (III-1) confirmed upon MCD at 2 years of age, and treated with angiotensin converting enzyme inhibitor (ACEI). Her proteinuria gradually increased, hence, a second kidney biopsy was performed at 10 years of age and confirmed identical to those from the first biopsy (Fig. 3Aa, b). Her treatment was changed to angiotensin II receptor blocker (ARB); her proteinuria was increased to nephrotic level at last follow up.

During proband's aunt (II-4) second pregnancy at 30 years of age, she developed nephrotic-range proteinuria, hematuria and hypertension. She was treated with ARB, however, her serum creatinine level was gradually increased. At 39 years of age, a kidney biopsy was performed, resulting in confirmation of focal segmental glomerulosclerosis (FSGS) (Fig. 3Ac, d). She was continued a therapy with ARB, with her estimated GFR maintaining 62.2 ml/min at 42 years of age.

Renal biopsy of her daughters (III-2 and III-3) was not performed in either instance and younger daughter (III-3) was also treated with ARB; her (III-3) proteinuria did not change and renal function has since maintained a normal level.

Renal histological analyses

Histological findings from kidney biopsies for II-2, II-4 and III-1 are summarized in

Table 2. Both the proband's (III-1) and mother's (II-2) renal histological examinations indicated MCD (Fig 3Aa, b), whereas, her aunt's biopsy (II-4) revealed FSGS (Fig 3Ac, d). None of the specimens demonstrated GBM abnormalities by light microscopy and no specific deposition of immunoglobulin or complements were detected by immunofluorescence microscopy. Focal foot process effacement was noticed by electron microscopy in both of proband's first and second biopsy and aunt's biopsy. Electron microscopy of first and second renal biopsy of III-1 revealed focal thinning of GBM, however, lucent or moth-eaten areas were not observed in an available sample (Fig. 3B). Tannic acid staining of first and second biopsy of III-I revealed fibrillar collagen material in the GBM by electron microscopy, and type III collagen was focally stained in glomeruli as indicated by immunofluorescence analysis (Fig. 4), indicating that tannic acid staining or immunofluorescence analysis is more sensitive for detecting fibrillar deposition in GBM than change of electron-lucent area by electron microscopy. Because podocin expression is regulated by LMX1B, we examined whether change of podocin expression is observed in early stage of the disease progression. While linear expression of podocin is observed in control samples, podocin expression was significantly decreased even in samples at 2 years of age (III-1) (Fig. 5). This change was also observed in proband's second renal biopsy

Discussion

Using WES, we identified heterozygous *LMX1B* R246Q mutation in a large family of nonsyndromic autosomal dominant nephropathy. Because skeletal and nail anomalies were not noticed and electron microscopy did not indicate a moth-eaten GBM appearance unique to NPS nephropathy, clinical findings and routine renal histology did not provide diagnostic suspicion of *LMX1B* mutation. Genetic investigations utilizing NGS technologies are useful in diagnosing familial nephropathy with uncertain cause. *LMX1B* is a strong candidate gene, capable of causing autosomal dominant renal-limited disease.

To date, *LMX1B* R246Q mutation has been reported only in two papers. Boyer *et al.* described two large families with *LMX1B* mutation without renal manifestation, however, detail and longitudinal clinical course of this disease were not clear[6]. Isojima *et al*. had reported a case with isolated nephropathy who had been tested for *LMX1B* mutation because of characteristic pathological findings such as moth-eaten appearance of GBM[5]. The present report is the first one, which describes long-term clinical course of proteinuria and renal function in a family with *LMX1B* R246Q.

Clinical observation for more than 10 years demonstrated that five out of six

affected patients in our family exhibit proteinuria without edema during early childhood. Chronological assessment of urinary abnormality or kidney function revealed proteinuria gradually increases to nephrotic levels in their adolescence. In all the affected patients, normal renal function is maintained throughout childhood, however, renal function gradually decreased and progressed to ESRD in adult patients (Fig. 3). The previously reported isolated case also maintained normal renal function at age of 9[5]. Furthermore, two patients out of twelve patients reported by Boyer was also diagnosed during their schoolage[6]. These findings suggested that a large fraction of patients with R246Q mutation might develop asymptomatic proteinuria or hematoproteinuria from early childhood. By childhood urinary screening, an early detection before renal function deterioration could be possible in at least a part of patients carrying R246Q mutation.

Boyer *et al.* reported eight (out of twelve) patients with R246Q mutation who progressed to chronic kidney disease (CKD) stage II-IV. Among them, five individuals had reached to ESRD [6]. Together with the present report, all the patients with R246Q in middle age or above have had decreased renal function. On the other hand, previous studies estimate renal failure occurs in about 5–10% of patients with typical NPS [1-4], and the severity of nephropathy is extremely variable both within and between families.

Therefore, renal prognosis with R246Q mutation may be poor compared with typical NPS, and progression to CKD may be inevitable without any medication.

Persistent severe proteinuria has often leads to loss of kidney function. Despite of the genetic causes, angiotensin-converting enzyme (ACE) inhibition has been demonstrated to be effective on the delay of disease progression in a variety of proteinuric glomerular diseases. For example, early diagnosis and renoprotective therapy with ACEI in oligosymptomatic patients with Alport syndrome could delay onset of ESRD [18]. These reports raise the possibility that treatment with ACE inhibitors might provide renoprotection in patients with LMX1B mutation. Indeed, Lemley reports effectiveness of ACEI and or ARB usage in NPS nephropathy[4]. Dramatic antiproteinuric effect in infantile nephrotic syndrome due to LMX1B mutation had also been demonstrated[19]. In the present report, three individuals (II-4, III-1 and III-3) have been treated with renin-angiotensin-aldosterone system (RAAS) inhibitors, such as ACEI and ARB. While one adult patient (II-4) has already been diagnosed as CKD stage II, the other two patients in their teens maintained renal function. Thus, a longitudinal study following a large number of patients is needed to clarify protective effects of RAAS inhibitors on renal prognosis of R246Q mutation.

In our investigation, kidney histology of two childhood patients demonstrated

MCD while that of an adult patients exhibited FSGS (table 2 and Fig. 3). In the previous reports, several patterns of pathology, such as MCD, FSGS and mesangial proliferative glomerulonephritis, were observed in patients manifesting renal-limited phenotypes of *LMX1B* mutation[5, 6, 20]. In this manner, light microscopy findings of this disease were variable possibly by the disease duration. Furthermore, irregular thickening of GBM with electron lucent areas were not always detected by electron microscopic examination [5, 6, 20]. Interestingly, despite a lack of moth-eaten appearance in our case, collagen fibrils within the GBM were detected by tannic acid staining of electron microscopy and type III collagen was focally stained in glomeruli by immunofluorescence microscopy. These results indicated that tannic acid staining or immunofluorescence analysis is more sensitive for detecting fibrillar deposition in GBM than change of electron-lucent area by electron microscopy. Therefore, collagen staining by electron and/or immunofluorescence microscopy may help diagnose *LMX1B* -associated nephropathy, especially in patients with autosomal dominant nephropathy with uncertain cause.

Studies on Lmx1b-null mice have demonstrated possible downstream targets of LMX1B as α3 and α4 type IV collagens, podocin and CD2AP[5, 21-24]. In vitro study also demonstrated that podocin expression is regulated combinatorially by Lmx1B and

FoxC[25]. However, in at least in some typical NPS patients with a thickened GBM and deposition of collagen Type III in the GBM, podocin protein expression was not altered indicating the possibility that decreased expression of podocin is secondary to podocyte injury, not by the primary effect of LMX1B on its transcription[26]. Notably, in our patient with R246Q mutation, podocin expression was significantly decreased compared with MCD from the first renal biopsy at 2 years of age. Although whether this change is general features in R246Q patients or not is still unclear, this case suggested that R246Q mutation affected podocyte slit diaphragm integrity even in early stage of the disease progression.

In conclusions, genetic analyses were helpful in autosomal dominant renal-limited disease to diagnose LMX1B-associated nephropathy, even in cases in which moth-eaten appearance was not confirmed by electron microscopy. Clinical manifestation can be variable, however by using the urinary screening examination, an early detection may be possible for renoprotective treatment to delay of disease progression. Furthermore, R246Q mutation results in subtle, but distinct podocyte damage in early stage, and manifest various types of histological alteration in adulthood, which finally leads to renal dysfunction.

Acknowledgements

This work was supported by grants from the Ministry of Health, Labour and Welfare (Yoshiura K); a Grant-in-Aid for Scientific Research (B) (Yoshiura K); the Japan Agency for Medical Research and Development (AMED) (Yoshiura K); and a Grant-in-Aid for Clinical Research from Miyazaki University Hospital (Konomoto T).

Conflict of interest: none

References

1 Bongers EM, Gubler MC, Knoers NV. Nail-patella syndrome. Overview on clinical and molecular findings. *Pediatr Nephrol*. 2002; **17**: 703-12.

2 Bongers EM, Huysmans FT, Levtchenko E, de Rooy JW, Blickman JG, Admiraal RJ*, et al.* Genotype-phenotype studies in nail-patella syndrome show that LMX1B mutation location is involved in the risk of developing nephropathy. *Eur J Hum Genet*. 2005; **13**: 935-46.

3 Sweeney E, Fryer A, Mountford R, Green A, McIntosh I. Nail patella syndrome: a review of the phenotype aided by developmental biology. *J Med Genet*. 2003; **40**: 153-62.

4 Lemley KV. Kidney disease in nail-patella syndrome. *Pediatr Nephrol*. 2009; **24**: 2345-54.

5 Isojima T, Harita Y, Furuyama M, Sugawara N, Ishizuka K, Horita S*, et al.* LMX1B mutation with residual transcriptional activity as a cause of isolated glomerulopathy. *Nephrol Dial Transplant*. 2014; **29**: 81-8.

6 Boyer O, Woerner S, Yang F, Oakeley EJ, Linghu B, Gribouval O*, et al.* LMX1B mutations cause hereditary FSGS without extrarenal involvement. *J Am Soc Nephrol*. 2013; **24**: 1216-22.

7 Kent WJ, Sugnet CW, Furey TS, Roskin KM, Pringle TH, Zahler AM*, et al.* The human genome browser at UCSC. *Genome Res*. 2002; **12**: 996-1006.

8 McKenna A, Hanna M, Banks E, Sivachenko A, Cibulskis K, Kernytsky A*, et al.* The Genome Analysis Toolkit: a MapReduce framework for analyzing next-generation DNA sequencing data. *Genome Res*. 2010; **20**: 1297-303.

9 Mishima H, Sasaki K, Tanaka M, Tatebe O, Yoshiura K. Agile parallel bioinformatics workflow management using Pwrake. *BMC Res Notes*. 2011; **4**: 331.

10 Wang K, Li M, Hakonarson H. ANNOVAR: functional annotation of genetic variants from high-throughput sequencing data. *Nucleic Acids Res*. 2010; **38**: e164.

11 Harrow J, Frankish A, Gonzalez JM, Tapanari E, Diekhans M, Kokocinski F*, et al.* GENCODE: the reference human genome annotation for The ENCODE Project. *Genome Res*. 2012; **22**: 1760-74.

12 Drmanac R, Sparks AB, Callow MJ, Halpern AL, Burns NL, Kermani BG*, et al.* Human genome sequencing using unchained base reads on self-assembling DNA nanoarrays. *Science*. 2010; **327**: 78-81.

13 Abecasis GR, Auton A, Brooks LD, DePristo MA, Durbin RM, Handsaker RE*, et al.* An integrated map of genetic variation from 1,092 human genomes. *Nature*. 2012; **491**: 56-65.

14 Bailey JA, Yavor AM, Massa HF, Trask BJ, Eichler EE. Segmental duplications: organization and impact within the current human genome project assembly. *Genome Res*. 2001; **11**: 1005-17.

15 Bailey JA, Gu Z, Clark RA, Reinert K, Samonte RV, Schwartz S*, et al.* Recent segmental duplications in the human genome. *Science*. 2002; **297**: 1003-7.

16 Vollrath D, Jaramillo-Babb VL, Clough MV, McIntosh I, Scott KM, Lichter PR*, et al.* Loss-of-function mutations in the LIM-homeodomain gene, LMX1B, in nail-patella syndrome. *Hum Mol Genet*. 1998; **7**: 1091-8.

17 Othman M. Platelet-type Von Willebrand disease: three decades in the life of a rare bleeding disorder. *Blood Rev*. 2011; **25**: 147-53.

18 Gross O, Licht C, Anders HJ, Hoppe B, Beck B, Tönshoff B*, et al.* Early angiotensin-converting enzyme inhibition in Alport syndrome delays renal failure and improves life expectancy. *Kidney Int*. 2012; **81**: 494-501.

19 Proesmans W, Van Dyck M, Devriendt K. Nail-patella syndrome, infantile nephrotic syndrome: complete remission with antiproteinuric treatment. *Nephrol Dial Transplant*. 2009; **24**: 1335-8.

20 Edwards N, Rice SJ, Raman S, Hynes AM, Srivastava S, Moore I*, et al.* A novel LMX1B mutation in a family with end-stage renal disease of 'unknown cause'.

Clin Kidney J. 2015; **8**: 113-9.

21 Miner JH, Morello R, Andrews KL, Li C, Antignac C, Shaw AS*, et al.* Transcriptional induction of slit diaphragm genes by Lmx1b is required in podocyte differentiation. *J Clin Invest*. 2002; **109**: 1065-72.

22 Morello R, Zhou G, Dreyer SD, Harvey SJ, Ninomiya Y, Thorner PS*, et al.* Regulation of glomerular basement membrane collagen expression by LMX1B contributes to renal disease in nail patella syndrome. *Nat Genet*. 2001; **27**: 205-8.

23 Rohr C, Prestel J, Heidet L, Hosser H, Kriz W, Johnson RL*, et al.* The LIM-homeodomain transcription factor Lmx1b plays a crucial role in podocytes. *J Clin Invest*. 2002; **109**: 1073-82.

24 Burghardt T, Kastner J, Suleiman H, Rivera-Milla E, Stepanova N, Lottaz C*, et al.* LMX1B is essential for the maintenance of differentiated podocytes in adult kidneys. *J Am Soc Nephrol*. 2013; **24**: 1830-48.

25 He B, Ebarasi L, Zhao Z, Guo J, Ojala JR, Hultenby K*, et al.* Lmx1b and FoxC combinatorially regulate podocin expression in podocytes. *J Am Soc Nephrol*. 2014; **25**: 2764-77.

26 Heidet L, Bongers EM, Sich M, Zhang SY, Loirat C, Meyrier A*, et al.* In vivo expression of putative LMX1B targets in nail-patella syndrome kidneys. *Am J Pathol*.

2003; **163**: 145-55.

Figure legends

Figure 1: Pedigree and *LMX1B* mutation. (A) Pedigree demonstrated an autosomal dominant pattern of disease, and included six affected patients over three generations. DNA is available from five patients (II-2, II-4, III-1, III-2 and III-3) and two unaffected relatives (II-1 and II-3). WES was performed in these seven persons. (B) Radiographs of pelvis (a) and knee (b) of proband (III-3). No iliac horn and patella dysplasia can be noticed. (C) *LMX1B* heterozygous G-to-A mutation in exon 4 (c.737G>A, p.R246Q) was confirmed by Sanger sequencing in all affected patients.

Figure 2: Progression of proteinuria and renal function. Urinary protein/creatinine ratio and serum creatinine level of patient (III-3, III-1 and II-4) were presented. Proteinuria was recognized in early childhood (III-3). Proteinuria gradually increases to nephrotic levels in their adolescence, and normal renal function is maintained in child patients (III-3 and III-1). Renal function gradually decreased and progressed in adult patients (II-4).

Figure 3: Kidney histology of child and adult patients. (A) Light microscopy of proband's (III-1) second biopsy and her aunt's (II-4) biopsy (Periodic acid-Schiff stain).

Patients III-1 (a and b) and II-4 (c and d) show a normal glomerulus and focal segmental glomerulosclerosis, respectively. (B) Electron microscopy of proband's (III-1) and her aunt's (II-4), (a) and (b) are first, (c) and (d) are second biopsy of III-1, and (e) and (f) are biopsy of II-4. Focal foot process effacement is noticed in both patients (red arrows). Focal thinning of GBM was observed on patient III-1 (a and c) and normal GBM on patient II-4 (e). Electron lucent areas in the GBM, referred to as a moth-eaten appearance, and most specific histological changes of NPS are not observed. Electron dense deposits are not present.

Figure 4: Collagen staining of the proband (III-1). Upper panel shows first biopsy specimens taken at an age of 2 years. Lower panel shows second biopsy specimens from 10 years of age. Collagen staining with tannic acid in electron microscopic examination indicates collagen fibrils in GBM (red arrows). Second lane is enlarged image of collagen fibrils. Type III collagen is focally expressed in glomeruli at both of first and second biopsy, however type I collagen is not observed.

Figure 5: Immunohistological analysis of podocin in glomeruli from the patient (III-1). Renal biopsy specimen of MCD patients is used as an age matched control of

proteinuric kidney disease. Lower panel is enlarged image. Podocin expression significantly decreases compared with control even in first biopsy samples at 2 years of age. Podocin expressions from the second biopsy are identical to those from the first.

A

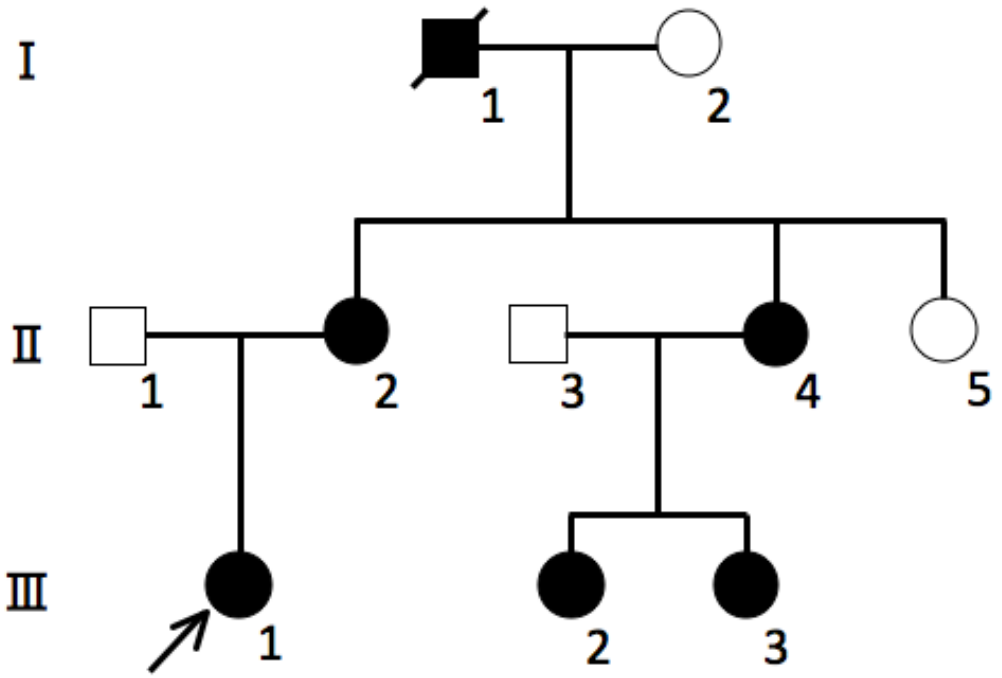

B

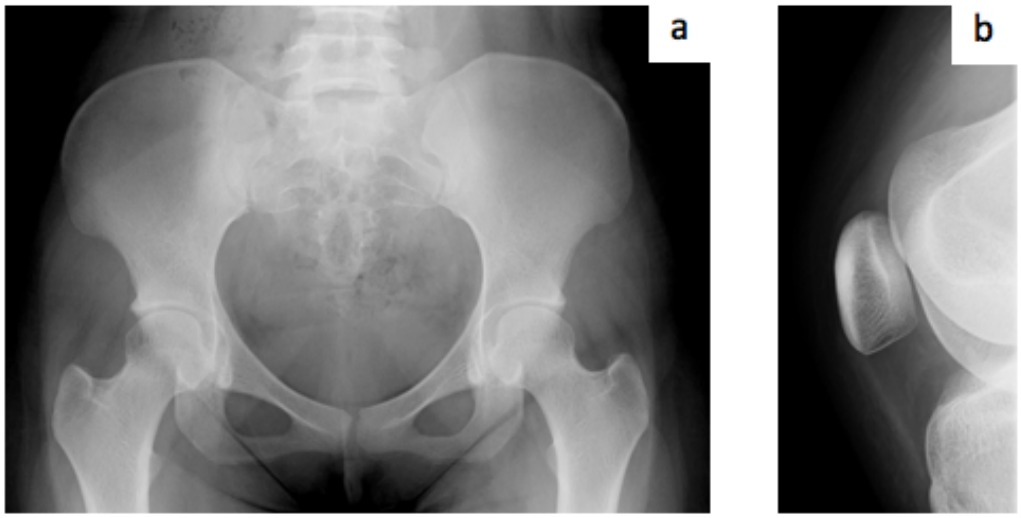

C

Patient

c.737G>A, p.R246Q

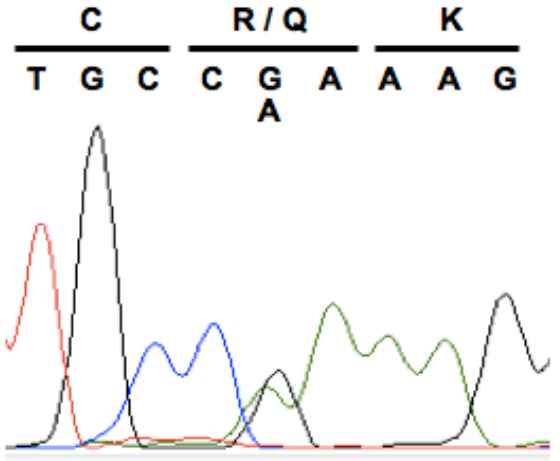

Unaffected

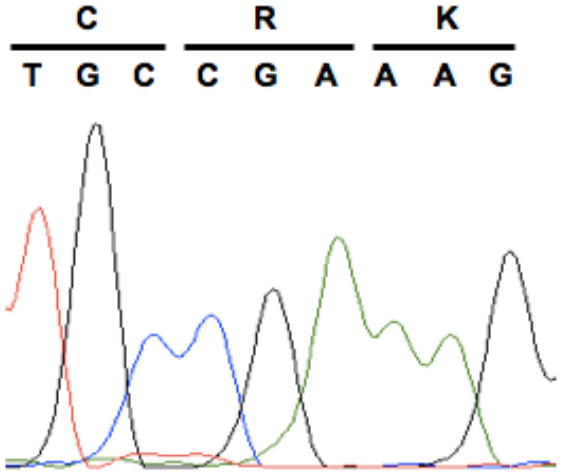

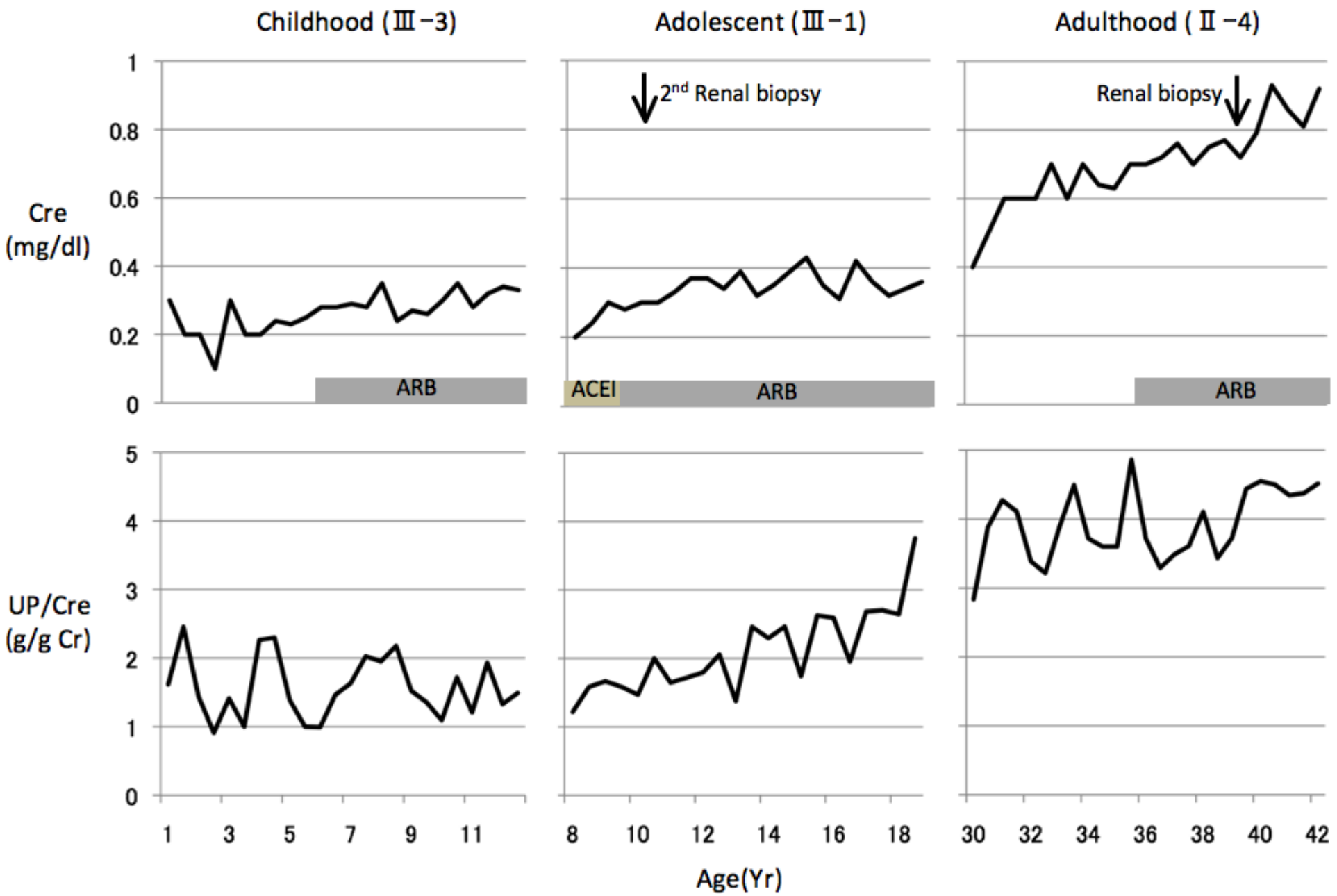
Childhood (Ⅲ-3)
Adolescent (Ⅲ-1)
Adulthood (Ⅱ-4)
2nd Renal biopsy
Renal biopsy
Cre (mg/dl)
UP/Cre (g/g Cr)
ARB
ACEI
ARB
ARB
1
0.8
0.6
0.4
0.2
0
5
4
3
2
1
0
1 3 5 7 9 11
8 10 12 14 16 18
30 32 34 36 38 40 42
Age(Yr)

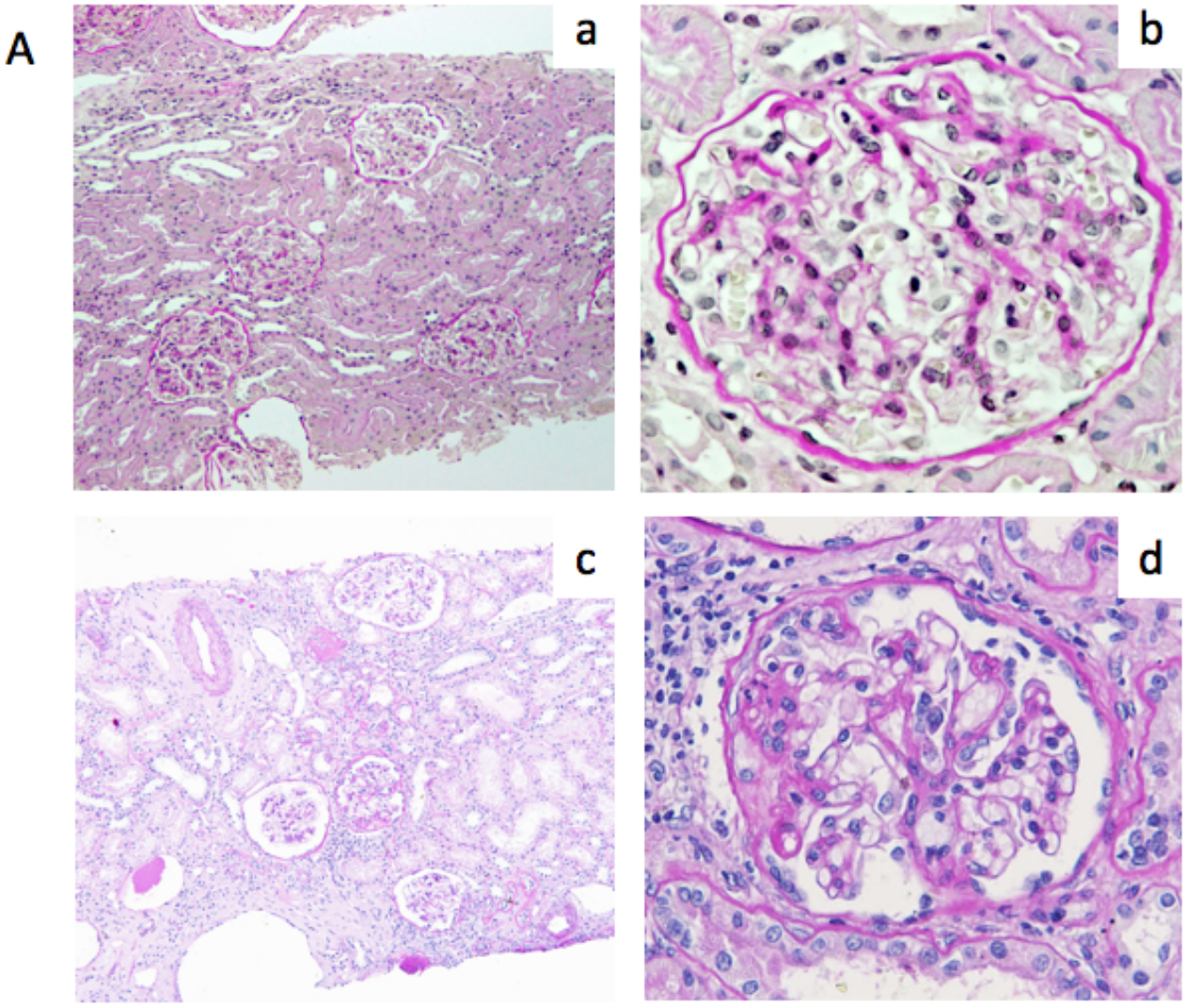
A
a
b
c
d

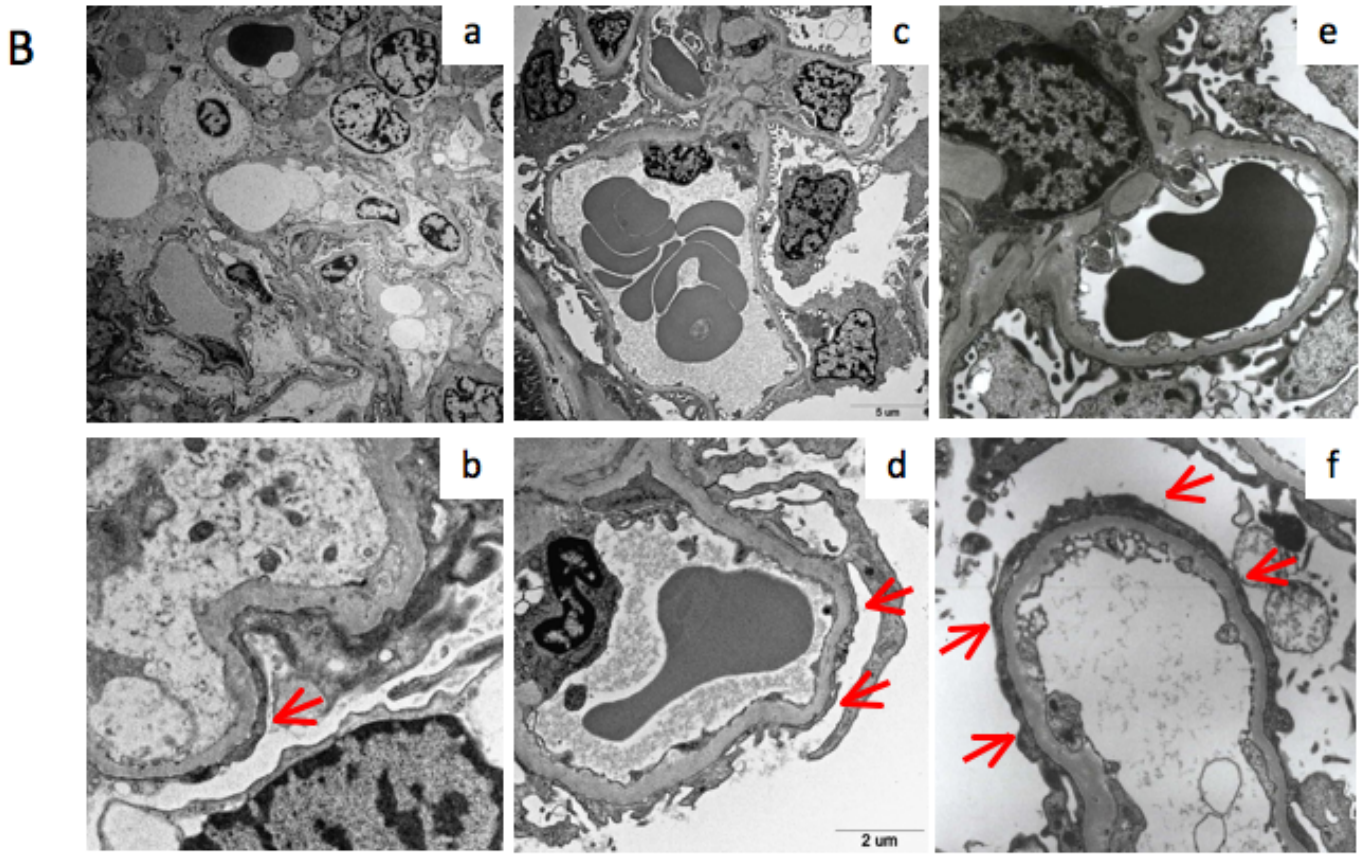
B
a
c
e
b
d
f
5 um
2 um

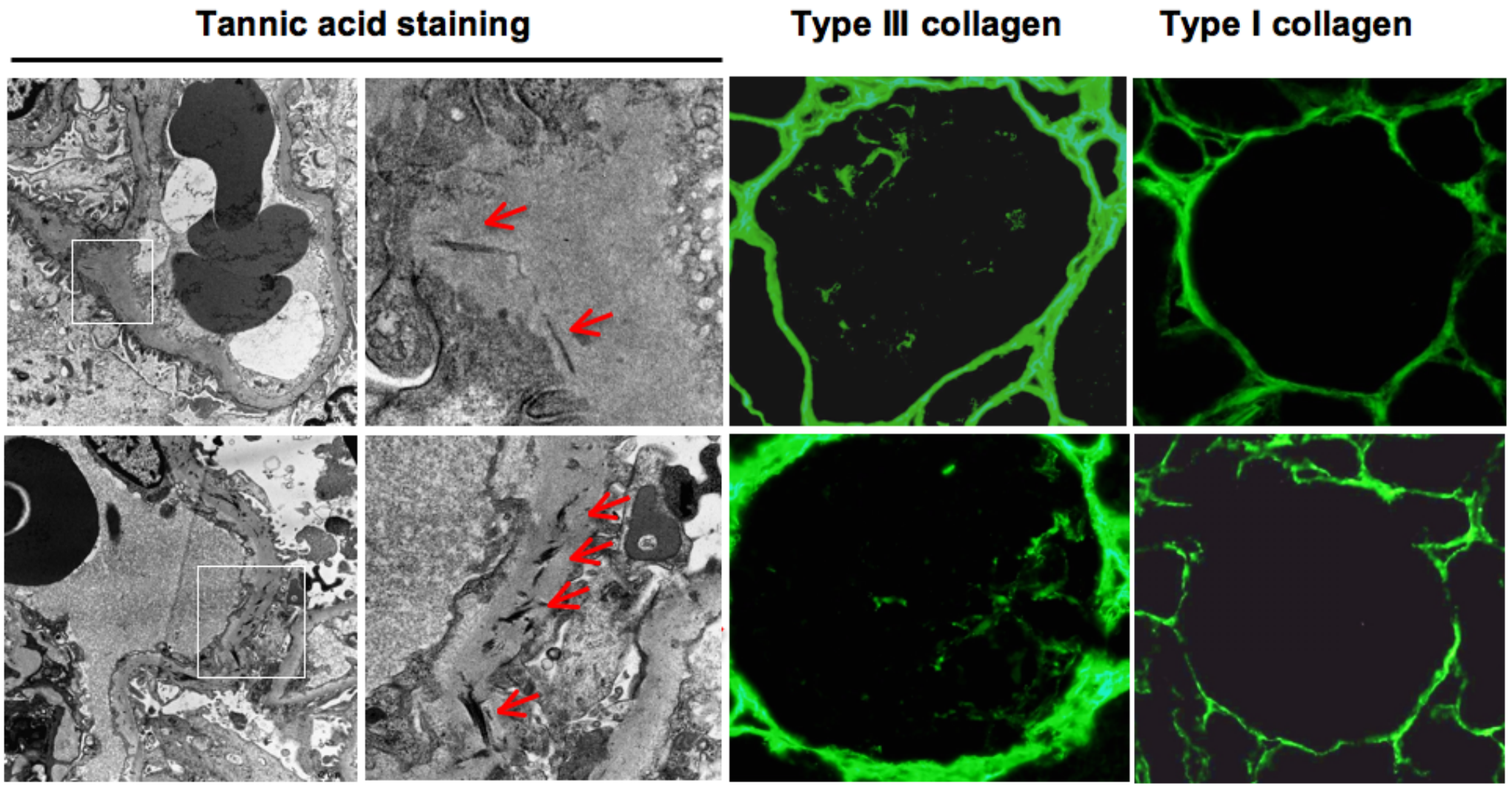
Tannic acid staining
Type III collagen
Type I collagen

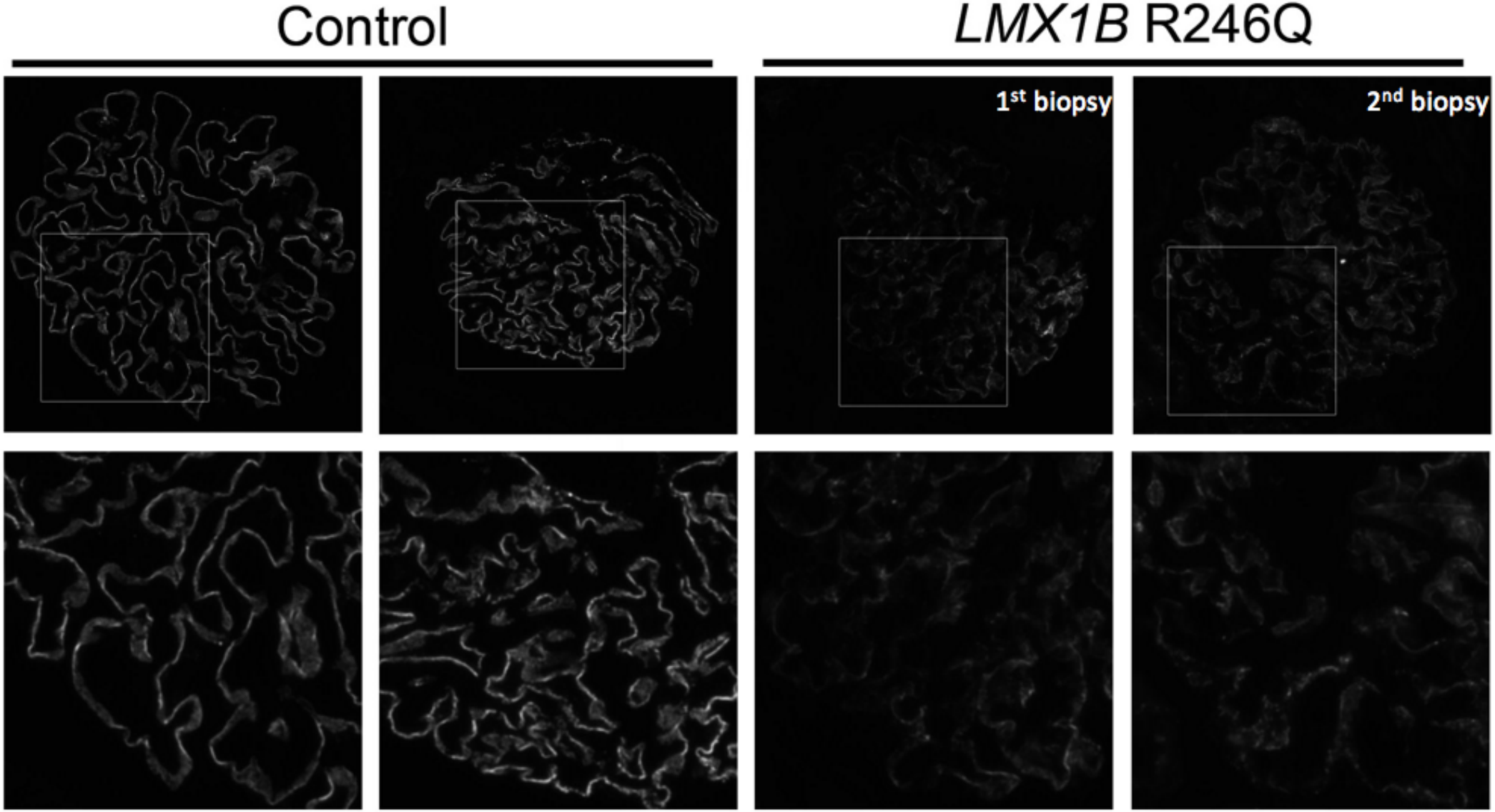
Control
LMX1B R246Q
1st biopsy
2nd biopsy

Supplementary Table 1. pathogenicity analysis of gene variants

	Ensembl ID	variant		Polyphen-2 (score)		SIFT (score)		PROVEAN (score)	
LMX1B	ENST00000526117	c.G737A	p.R246Q	probably damaging	0.983	Damaging	0.02	deleterious	−3.91
TMEM51	ENST00000376008	c.G74C	p.G25A	probably damaging	0.999	Damaging	0	deleterious	−5.08
LACTBL1	ENST00000426928	c.A70G	p.T24A	benign	0	N/A	N/A	neutral	−0.66
UBR3	ENST00000272793	c.A4556T	p.Q1519L	benign	0	tolerated	0.27	neutral	−2.46
TRIM42	ENST00000286349	c.G1398C	p.Q466H	benign	0	tolerated	0.56	neutral	−0.76
GIN1	ENST00000399004	c.A1465G	p.R489G	benign	0.058	Damaging *	0	neutral	−1.12
SH3TC2	ENST00000538184	c.G1954A	p.V652M	benign	0.196	tolerated	0.09	neutral	−1.92
IDO2	ENST00000502986	c.A458T	p.K153I	benign	0.312	N/A	N/A	deleterious	−6.37
GLI4	ENST00000340042	c.A758G	p.H253R	possibly damaging	0.626	tolerated	0.68	deleterious	−4.09
ZIC5	ENST00000267294	c.1260_1262del	p.420_421del	N/A	N/A	N/A	N/A	neutral	0.84
GP1BA	ENST00000329125	c.1273_1311del	p.425_437del	N/A	N/A	N/A	N/A	deleterious	−11.21

Polyphen-2 (HumVar) score: range 0-1.0 1.0 being most deleterious
SIFT score: range 0-1.0, 0 being most deleterious
PROVEAN score: cutoff -2.5, lower score being deleterious
N/A, not applicable; *Low confidence.

Table 1. Clinical findings of *LMX1B* R246Q mutation

Patient	Age at Onset (yr)	Extra Renal Feature	At onset			At Last Follow-up or At induction of HD			
			Proteinuria Dipstick or g/g Cr	Hematuria Dipstick	edema	Proteinuria (g/g Cr)	Hematuria Dipstick	Albumin (g/dL)	eGFR (ml/min/1.73m^2) and Age (yr)
I-1	Unknown	-	ND	ND	ND	ND	ND	ND	ESRD at 40
II-2	6	-	+++	+	-	9.5	+	3.43	ESRD at 38
II-4	13	-	++	-	-	4.5	+	2.95	62.2 at 42
III-1	1	-	+++	+++	-	3.7	++	2.78	187.6 at 18
III-2	11	-	++	-	-	0.8	+	2.99	154.9 at 15
III-3	1	-	1.6	+	-	1.5	++	2.40	161.1 at 12

ND, not determined; HD, hemodialysis; ESRD, end stage renal disease

Table 2. Kidney histology of *LMX1B* R246Q mutation

Patient	Age at Renal biopsy (yr)	Kidney Histology		
		LM	IF	EM
Ⅱ-2	15	MCD without TI change	No deposition	ND
Ⅱ-4	39	FSGS with focal interstitial fibrosis and tubular atrophy	No deposition	Focal foot process effacement Moth-eaten appearance (-)
Ⅲ-1 (1st)	2	MCD without TI change	No deposition	Focal foot process effacement Focal thinning of GBM Moth-eaten appearance (-)
Ⅲ-1 (2nd)	10	MCD without TI change	No deposition	Focal foot process effacement Focal thinning of GBM Moth-eaten appearance (-)

LM, light microscopy; IF, Immunofluorescence microscopy; EM; electron microscopy; MCD, minimal change disease; FSGS, focal segmental glomerulosclerosis; TI change, tubulo-interstitial change; GBM, glomerular basement membrane; ND, not determined